

# The optical spectrum of PKS 1222+216 and its black hole mass

E. P. Farina<sup>1\*</sup>, R. Decarli<sup>2</sup>, R. Falomo<sup>3</sup>, A. Treves<sup>1,4</sup>, and C. M. Raiteri<sup>5</sup>.

<sup>1</sup> *Università degli Studi dell’Insubria, via Valleggio 11, I-22100 Como, Italy*

<sup>2</sup> *Max-Planck-Institut für Astronomie, Königstuhl 17, D-69117 Heidelberg, Germany*

<sup>3</sup> *INAF – Osservatorio Astronomico di Padova, Vicolo dell’Osservatorio 5, I-35122 Padova (PD), Italy*

<sup>4</sup> *Associated to INAF and INFN*

<sup>5</sup> *INAF – Osservatorio Astronomico di Torino, Via Osservatorio 20, I-10025 Pino Torinese (TO), Italy*

## ABSTRACT

We investigate the optical spectral properties of the blazar PKS 1222+216 during a period of  $\sim 3$  years. While the continuum is highly variable (i.e., from  $\lambda L_\lambda(5100\text{\AA}) \sim 3.5 \times 10^{45}$  erg/s up to  $\sim 15.0 \times 10^{45}$  erg/s) the broad line emission is practically constant. This supports a scenario in which the broad line region is not affected by jet continuum variations. We thus infer the thermal component of the continuum from the line luminosity and we show that it is comparable with the continuum level observed during the phases of minimum optical activity. The mass of the black hole is estimated through the virial method from the FWHM of Mg II, H $\beta$ , and H $\alpha$  broad lines and from the thermal continuum luminosity. This yields a consistent black hole mass value of  $\sim 6 \times 10^8 M_\odot$ .

**Key words:** galaxies: active — quasars: individual: PKS 1222+216

## 1 INTRODUCTION

PKS 1222+216 (also known as 4C +21.35;  $z = 0.432$ ;  $r \sim 16$ ; Burbidge & Kinman 1966; Osterbrock & Pogge 1987) is a Flat Spectrum Radio Quasar (FSRQ). At radio wavelengths it exhibits a peculiar bended large scale ( $\sim 100$  kpc) structure and an apparent superluminal motion has been noticed in mas-scale subcomponents of its jet (e.g., Hooimeyer et al. 1992). In X-rays a counterpart was found by ROSAT (Brinkmann, Yuan, & Siebert 1997), and in  $\gamma$ -rays by EGRET (Hartman et al. 1999).

In the high energy range, PKS 1222+216 has recently shown a particularly active behaviour with flares also in the Very High Energy domain (VHE, i.e.  $E > 100$  GeV). In April 2009 a first outburst was reported by the Fermi Large Area Telescope (Longo, Giroletti, & Iafate 2009) followed, in December 2009, by a larger one observed by both the AGILE Gamma-ray Imaging Detector (Verrecchia et al. 2009) and Fermi (Ciprini 2009). A further flare in April 2010 reached the VHE (Donato 2010). This triggered several observations in the TeV region with the ground based Cherenkov telescopes VERITAS and MAGIC, which were unsuccessful. The source was finally detected with MAGIC in June 2010 (Mariotti 2010; Aleksić et al. 2011), in coincidence with a second huge GeV emission recorded by AGILE and Fermi (Striani et al. 2010; Iafate, Longo, & D’Ammando

2010; Tanaka et al. 2011). PKS 1222+216 is the third FSRQ, after 3C279 ( $z=0.536$ ) and PKS 1510-089 ( $z=0.36$ ), observed at such high energy. The 30 minutes observation by MAGIC allows a measurement of a variability time-scale of about 10 minutes. The spectral energy distribution of the object and the high variability imply that the jet is relativistic with large beaming factors. Tavecchio et al. (2011) suggest that the origin of the rapidly variable VHE energy emission arose in a small region outside the Broad Line Region (BLR): if this emission were produced within the BLR, the high energy photons would be strongly absorbed by photons from emission lines (see also Böttcher, Reimer, & Marscher 2009; Nalewajko et al. 2012). Alternatively a more exotic scenario that considers photon/axion transition was proposed by Tavecchio et al. (2012).

The optical and NIR emission of PKS 1222+216 had shown high daily fluctuations, that are not always related to the  $\gamma$ -ray variability (e.g., Carrasco et al. 2010; Hauser, Wagner, & Hagen 2010; Nesci & Montagni 2010; Smith, Schmidt, & Jannuzi 2011).

In this paper we analyse the optical observations of PKS 1222+216. We study the variability of both continuum and emission lines. From the lines luminosity we deduce the thermal continuum and contrast it with the highly variable jet component. Finally we estimate the virial mass of the black hole from different recipes and lines (i.e., Mg II, H $\beta$ , and H $\alpha$ ) and compare it with the literature results.

\* E-mail: emanuele.farina@mib.infn.it

Throughout this paper we consider a concordance cosmology with  $H_0 = 70$  km/s/Mpc,  $\Omega_m = 0.3$ , and  $\Omega_\Lambda = 0.7$ .

## 2 OPTICAL SPECTROSCOPY

Spectrophotometry with the Hawaii 2.2m telescope was presented by Stockton & MacKenty (1987) who however reported only line and continuum intensities. The source was observed between 3900Å and 9100Å within the Sloan Digital Sky Survey (SDSS; York et al. 2000) in January 2008 and the spectrum is reported in Figure 1.

Optical spectrophotometry and polarimetry was performed at the Steward Observatory with the 2.3m Bok and 1.54m Kuiper telescopes (Smith et al. 2009; Smith, Schmidt, & Jannuzi 2011). All the data are accessible to the astronomical community<sup>1</sup>. Here we consider the 112 spectra obtained to date in the spectral range 4000Å–7550Å, calibrated through V photometry and not corrected for telluric absorptions. At wavelengths higher than  $\sim 7000$ Å, a strong fringing affects the spectra and prevents a precise analysis of the [OIII] $_{\lambda 5007}$  narrow line. Two examples of these spectra are reported in Figure 1.

We also retrieved some unpublished optical photometry collected between 1995 and 2001<sup>2</sup>. The data were acquired with the 105 cm REOSC telescope of the Torino Observatory, equipped with standard Johnson’s B, V, and Cousins’ R filters and a 1242 × 1152 pixel CCD (EEV) with a 0.467"/pixel scale until 2000, and with a 2048 × 2164 pixel CCD (Loral) with a 0.32"/pixel scale thereafter. Frames were reduced with canonical procedures and the source magnitude calibration was derived with respect to the photometric sequence published in Raiteri et al. (1998).

Triggered by the MAGIC detection, we observed the source with the 3.58m Telescopio Nazionale Galileo (TNG), La Palma, during the night of January 3, 2011. We used DOLORES (Device Optimised for the LOw RESolution, Molinari, Conconi, & Pucillo 1997) in spectroscopy configuration with the 2048×2048 pixel detector. Observations were carried out with LR–R grism, yielding a spectral resolution of  $R=714$  (1" slit) in the nominal spectral range 4470Å–10073Å ( $\Delta\lambda/\text{pxl}=2.61\text{Å}/\text{pxl}$ ). During the 1050 s of total exposure time the mean seeing was 1.0" and the transparency was not optimal. Standard IRAF<sup>3</sup> tools were used in the data reduction. The `ccdred` package was employed to perform bias subtraction, flat field correction, image alignment and combination. The accuracy in the wavelength calibration is around 0.17Å. Galactic extinction was accounted for according to Schlegel, Finkbeiner, & Davis (1998,  $E(B-V)=0.023$  mag). Telluric absorption bands were corrected with two spectrophotometric standard stars. One observed immediately after PKS 1222+216, and one collected with the same telescope configuration but in better weather conditions, on January 6, 2011. The feature at

$\sim 7200$ Å coincidentally corresponds to the [OIII] $_{\lambda 5007}$  emission at the redshift of the blazar, affecting the measure of this line. Investigating the region over 8000Å, where the H $\alpha$  line resides, is delicate due to a number of factors: the response function of LR–R presents a strong local decrease and an apparent fringing is superimposed to the spectra. Moreover the strong water vapour absorption feature at 9360 Å falls within the H $\alpha$  broad line. The flux calibration was performed through the photometry obtained at Steward observatory which has been interpolated within few hours. The spectrum obtained (average Signal-to-Noise ratio S/N  $\sim 30$ ) is presented in Figure 1.

For the analysis of spectroscopic data we followed the procedure presented in Decarli et al. (2010) and De Rosa et al. (2011). Namely, we have first subtracted the continuum designed as a superposition of: (i) the non thermal component modelled with a power-law, (ii) the host galaxy emission (adopting the Elliptical galaxy model by Mannucci et al. 2001), and (iii) the Fe II multiplets (from the template of Vestergaard & Wilkes 2001 in the UV band and from our original spectrum of IZw001 in optical). Broad emission lines have been fitted with two Gaussian curves with the same central wavelength (see Decarli et al. 2008), assuming the contribution of the narrow component as negligible. Errors on the estimated parameters have been derived considering the  $1\sigma$  uncertainties from both line and continuum fits.

The analysis of Steward observatory spectra required particular care. For this data we have fitted the continuum excluding the region beyond 7000Å, where the fringing dramatically decreases the quality of the spectra. The luminosity of the continuum at 5100Å was estimated by extrapolating the power-law up to this value. In order to not underestimate the measures of the H $\beta$  flux and FWHM the fit was performed excluding the region between 6850Å and 6930Å where the strong O<sub>2</sub> atmospheric feature affects the blue wing of the emission line.

In Table 1 we report the continuum luminosity at 3000Å and 5100Å, the luminosity and FWHM of Mg II, H $\beta$ , and H $\alpha$  when present. Relevant data from analysis of each Steward observatory spectrum are in Table 2.

## 3 THERMAL CONTINUUM AND BLACK HOLE MASS

In the usual unification scheme of AGNs (e.g., Urry & Padovani 1995), the relativistic jet of a blazar is viewed closely along the observer line of sight. Thus, the continuum in radio to optical/UV spectral range is dominated by a highly polarised non-thermal synchrotron radiation emitted by the energetic electrons in the jet superimposed to the thermal emission associated to the disk (e.g., Konigl 1981; Urry & Mushotzky 1982, and specifically for PKS 1222+216 Smith, Schmidt, & Jannuzi 2011).

In the last three years covered by the data, the continuum luminosity at 5100Å varied in the range  $35\text{--}150 \times 10^{44}$  erg/s. The REOSC photometry, collected before 2003, corresponds to a status of minimum activity ( $V \sim 16.1$ ). From these data we infer an average colour index  $(B - R) = 0.21 \pm 0.04$  which, assuming a power-law

<sup>1</sup> <http://james.as.arizona.edu/~psmith/Fermi/>

<sup>2</sup> Data available at:

<http://www.dfm.uninubria.it/farina/pks1222.html>

<sup>3</sup> IRAF is distributed by the National Optical Astronomy Observatories, which are operated by the Association of Universities for Research in Astronomy, Inc., under cooperative agreement with the National Science Foundation.

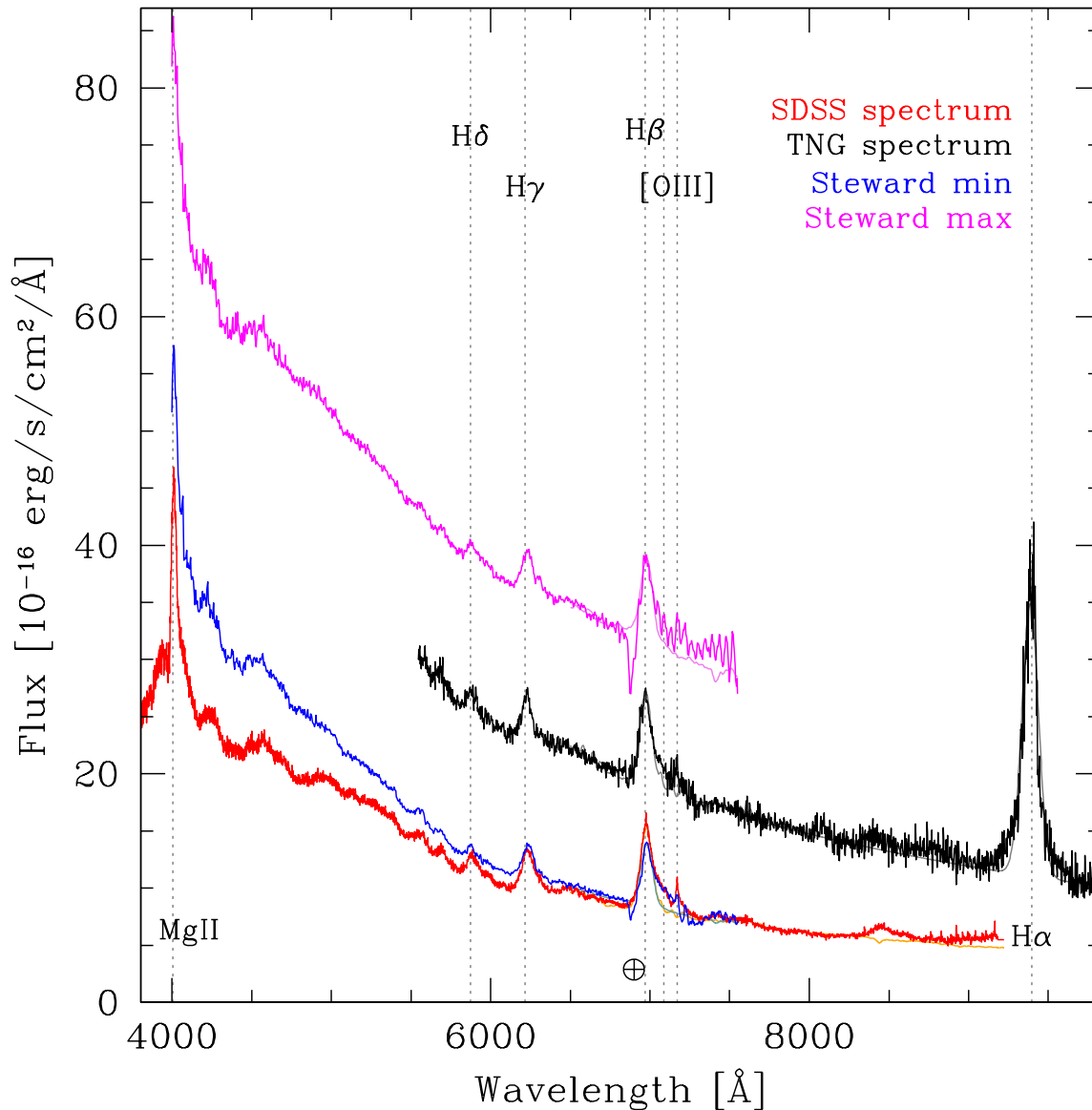


**Figure 1.** Dereddened spectra of PKS 1222+216 from: SDSS (red line), TNG (black solid line) and Steward observatory in correspondence of minimum (blue line) and maximum (magenta line) optical activity. The results of our fitting procedure on  $H\beta$  and  $H\alpha$  broad line are plotted in light colors. Most prominent emission lines are marked with grey dotted vertical lines and the  $\oplus$  symbol highlights the strong telluric absorption that affects the Steward observatory spectra at  $\sim 6900\text{\AA}$ . A colour version of this figure is available in the electronic edition of MNRAS.

optical spectrum  $F_\nu \propto \nu^{-\alpha}$ , translates into a spectral index  $\alpha = -0.44$ . This implies a flat optical spectrum in the  $\log F_\nu$  versus  $\log \nu$  plot, suggesting a prevailing contribution of thermal emission from the accretion disc over the synchrotron one.

Smith, Schmidt, & Jannuzi (2011) have shown that the  $H\beta$  luminosity in the Steward observatory sample is practically constant while the continuum is highly variable (see Figure 2). This is in good agreement with the SDSS and TNG spectra (see Figure 3). The  $H\beta$  luminosity mean value is  $45 \times 10^{42}$  erg/s with an rms of  $6 \times 10^{42}$  erg/s. As noted by Smith, Schmidt, & Jannuzi (2011) the constancy of the  $H\beta$  line indicates that the broad line region is marginally affected by the huge variability of the jet. This conclusion is

confirmed by our analysis that consider a larger number of spectra.

In order to evaluate the mass of the black hole we consider the virial approach by assuming the FWHM as a measure of the virial velocity and the thermal continuum luminosity as a proxy for the distance of the clouds from the black hole, since the observed continuum may be dominated by the jet emission. We calculate the thermal continuum through the relation with broad line luminosities found on QSOs (e.g., Greene & Ho 2005; Vestergaard & Peterson 2006; Decarli, Dotti, & Treves 2011). We calibrate the ratio for  $H\beta$  and continuum at  $5100\text{\AA}$  basing on the Shen et al. (2011) QSO property catalogue. The low luminosities objects ( $\log \lambda L_\lambda(5100\text{\AA}) < 44.5$ ) show a significant contami-

**Table 1.** Continuum luminosity, luminosities and FWHM of broad emission lines obtained from TNG and SDSS spectra. For the Steward observatory spectra, we quote the range of the variability of the continuum and of black hole mass, and the average value (with rms as uncertainty) of  $H\beta$  measurements. The black hole masses shown are the average values obtained following the recipes presented in §3.

	TNG spectrum Jan. 3, 2011	Steward observatory spectra Apr. 27, 2009 – July 27, 2011	SDSS spectrum Jan. 14, 2008
$\lambda L_\lambda(5100\text{\AA})$	$(88 \pm 2) \times 10^{44}$ erg/s	$[35 - 150] \times 10^{44}$ erg/s	$(35 \pm 1) \times 10^{44}$ erg/s
$\lambda L_\lambda(3000\text{\AA})$	...	...	$(60 \pm 1) \times 10^{44}$ erg/s
L( $H\alpha$ )	$(140 \pm 30) \times 10^{42}$ erg/s	...	...
L( $H\beta$ )	$(47 \pm 5) \times 10^{42}$ erg/s	$(45 \pm 6) \times 10^{42}$ erg/s	$(45 \pm 2) \times 10^{42}$ erg/s
L(Mg II)	...	...	$(94 \pm 6) \times 10^{42}$ erg/s
FWHM( $H\alpha$ )	$(2700 \pm 400)$ km/s	...	...
FWHM( $H\beta$ )	$(3600 \pm 250)$ km/s	$(3750 \pm 480)$ km/s	$(3750 \pm 50)$ km/s
FWHM(Mg II)	...	...	$(3600 \pm 90)$ km/s
$M_{\text{BH}}(H\alpha)$	$3.9 \times 10^8 M_\odot$	...	...
$M_{\text{BH}}(H\beta)$	$5.0 \times 10^8 M_\odot$	$[5.0 - 11.4] \times 10^8 M_\odot$	$5.4 \times 10^8 M_\odot$
$M_{\text{BH}}(\text{Mg II})$	...	...	$8.3 \times 10^8 M_\odot$

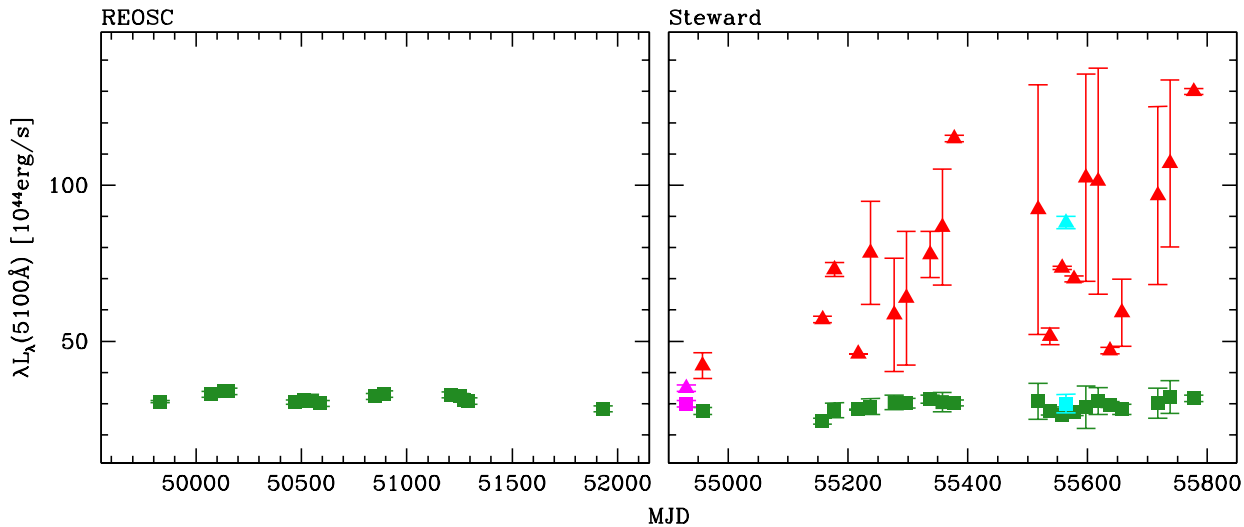


**Figure 2.** Luminosity of the measured continuum (triangle) and of the thermal component (squares) as a function of time. In the *Left Panel* we present data deduced from the REOSC photometry assuming an average spectral index  $\alpha = -0.44$  (see §3). These correspond to a status of minimum optical activity of the FSRQ. The *Right Panel* shows the measures from Steward observatory spectra (red filled triangle: continuum measured at 5100 Å, and green filled squares: thermal continuum calculated from  $H\beta$  luminosity). Cyan points are from TNG spectrum, and the magenta ones from SDSS (for the sake of clarity, this latter, observed the MJD(SDSS)=54479, is shifted at MJD=54925). Steward observatory and REOSC data are resampled in 20 days bins, and the plotted errors are the standard deviations. Uncertainties on the SDSS and TNG thermal continuum luminosities are the rms of the relation presented in §3.

nation from the host galaxy and thus are removed from the analysis. A similar cut is applied also to the luminosity of the lines, since faint lines are less reliable due to the contaminations from narrow emission. Average and rms values of the ratio are:

$$\log \frac{\lambda L_\lambda(5100\text{\AA})}{L(H\beta)} = 1.82 \pm 0.22 \quad (1)$$

The thermal continuum deduced from  $H\beta$  line luminosity ( $\sim 30 \times 10^{44}$  erg/s with an rms of  $3 \times 10^{44}$  erg/s) corresponds to the lower observed states of Table 1 (see Figure 2). The

virial mass can be expressed as:

$$\log \left( \frac{M_{\text{BH}}}{M_\odot} \right) = a \log \left( \frac{\text{FWHM}}{1000 \text{ km/s}} \right) + b \log \left( \frac{L_{\text{line}}}{10^{42} \text{ erg/s}} \right) + c \quad (2)$$

where the coefficients  $a$ ,  $b$ , and  $c$ , calibrated on local AGN with an estimate of the mass through the reverberation mapping technique, depend on the broad line considered. The uncertainties associated to these measures of the mass are very large ( $\gtrsim 0.4$  dex) and are dominated by the dispersion of the relations between the radius of the BLR and the thermal continuum luminosity (e.g., Vestergaard & Peterson 2006; Shen et al. 2011). In order to compare differ-

**Table 2.** For each Steward spectra we list the measure of continuum luminosity at 5100Å  $\lambda L_\lambda$ , luminosity (L), and FWHM of H $\beta$  broad line, and thermal continuum estimated from H $\beta$  luminosity (L(H $\beta$ )).

Date	$\lambda L_\lambda$ [ $10^{44}$ erg/s]	L [ $10^{42}$ erg/s]	FWHM [km/s]	$\lambda L_\lambda$ (H $\beta$ ) [ $10^{44}$ erg/s]	Date	$\lambda L_\lambda$ [ $10^{44}$ erg/s]	L [ $10^{42}$ erg/s]	FWHM [km/s]	$\lambda L_\lambda$ (H $\beta$ ) [ $10^{44}$ erg/s]
2009/04/27	45±1	41± 3	3945± 86	27	2010/05/16	60±1	44± 5	3604±428	29
2009/04/29	44±1	43± 4	4288±172	28	2010/05/17	71±2	39± 6	3263±684	26
2009/04/30	44±1	44± 3	4288± 86	29	2010/05/20	75±2	42± 7	3433±599	27
2009/05/01	43±1	41± 2	3947±172	27	2010/06/10	76±2	43± 7	3941±684	29
2009/05/02	35±1	40± 2	4288±342	27	2010/06/11	74±2	51± 6	4455±171	33
2009/11/17	57±2	37± 5	3436±172	24	2010/06/12	70±2	48± 6	4466±258	31
2009/12/15	74±1	42± 5	3948±173	28	2010/06/13	71±2	49± 7	4294±173	33
2009/12/17	70±1	45± 5	3946±259	30	2010/06/14	68±1	49± 6	4289±172	32
2009/12/18	73±1	46± 5	3778± 86	30	2010/06/15	75±2	46± 5	4294±173	30
2009/12/19	72±1	37± 4	2922±171	24	2010/06/16	87±1	45± 6	3950±429	30
2009/12/20	76±1	42± 4	3264±172	28	2010/07/07	83±2	38± 6	3605±600	25
2010/01/14	46±1	43± 5	3950±428	28	2010/11/10	52±1	49± 6	4122±515	33
2010/01/15	46±1	42± 3	3949±601	28	2010/11/11	53±2	47± 6	3779±428	31
2010/02/13	114±2	41± 7	3947±429	27	2010/11/12	53±2	49± 3	3607±344	33
2010/02/14	117±2	42± 7	3948±515	28	2010/11/13	53±2	41± 3	3265± 86	27
2010/02/15	117±3	49± 8	4288±172	33	2010/11/15	49±2	48± 3	3951±172	32
2010/02/15	118±4	61± 9	4800±343	40	2010/12/01	41±1	45± 7	3946±230	30
2010/02/15	121±3	57± 9	4630±342	38	2010/12/02	45±1	42± 6	3605±429	28
2010/02/16	110±2	51± 9	4289±513	33	2010/12/05	54±1	42± 5	3434±172	28
2010/02/16	114±3	54± 9	4460±343	36	2010/12/08	51±1	43± 3	3436±257	29
2010/02/16	115±2	46±10	4288±515	30	2010/12/09	49±1	45± 6	3264±258	30
2010/02/17	116±3	52± 7	4288±257	35	2011/01/02	90±2	49± 4	4118±427	33
2010/02/17	125±2	41± 8	3947±428	27	2011/01/04	75±2	52± 3	4118±172	34
2010/02/17	117±2	48± 6	4291±172	32	2011/01/08	104±2	48± 5	4289± 86	32
2010/02/18	130±2	48±10	4459±429	32	2011/02/02	50±1	43± 2	3265± 87	28
2010/02/18	119±2	59± 8	4799±257	39	2011/02/03	50±1	44± 2	3437±121	29
2010/02/19	120±3	52± 5	4458±310	34	2011/02/05	50±1	45± 3	3609±344	30
2010/02/19	128±2	41±10	3775±598	27	2011/02/07	49±1	43± 3	3437±343	28
2010/03/15	48±1	42± 5	3779±600	28	2011/02/08	50±1	43± 2	3609±173	29
2010/03/15	49±1	40± 6	3263±258	27	2011/03/02	129±3	49± 6	3953±428	32
2010/03/16	50±1	42± 6	3607±429	28	2011/03/04	143±2	43± 7	3433±428	28
2010/03/16	48±1	41± 6	3603±343	27	2011/03/04	152±2	39± 6	3261±343	26
2010/03/17	47±1	45± 9	4289±514	30	2011/03/05	120±3	60± 8	4288±599	40
2010/03/17	48±1	40± 6	3607±258	26	2011/03/05	121±3	62± 7	4632±257	41
2010/03/18	51±1	43± 8	3605±428	28	2011/03/06	129±2	43± 7	2919±343	28
2010/03/18	50±1	43± 4	3948±428	29	2011/03/06	131±2	42±11	2920±428	28
2010/03/19	53±1	46± 5	3607±344	31	2011/03/08	115±2	38± 6	3263±429	25
2010/03/19	52±1	41± 6	3435±257	27	2011/03/29	55±2	48± 4	4290±256	32
2010/03/20	54±1	42± 4	3774±428	28	2011/03/30	58±3	51± 7	4289±599	33
2010/03/20	53±1	45± 3	3259±174	29	2011/04/04	58±1	45± 4	3609±172	29
2010/03/21	51±1	43± 5	3779±428	28	2011/04/05	58±3	45± 5	3090±343	30
2010/03/21	55±1	41± 6	3435±429	27	2011/04/06	54±2	48± 7	2746±600	31
2010/04/05	73±1	38± 8	3262±258	25	2011/04/08	56±2	44± 5	3261±257	29
2010/04/05	74±2	40± 6	3606±515	26	2011/05/26	72±2	44± 5	3265±172	29
2010/04/06	73±2	44± 6	3945±685	29	2011/05/27	73±2	47± 5	3431±598	31
2010/04/06	73±3	40± 5	3262±172	26	2011/05/28	72±1	47± 3	3433±428	31
2010/04/07	73±2	39± 5	3263±172	26	2011/05/29	74±2	45± 4	4120±256	30
2010/04/07	70±1	41± 7	3606±258	27	2011/05/30	70±2	48± 4	3776±686	32
2010/04/08	69±2	41± 6	3606±429	27	2011/06/14	87±2	48± 5	3088±172	32
2010/04/09	74±1	45± 7	3948±514	29	2011/06/15	80±2	49± 4	3263±684	33
2010/04/09	74±2	39± 6	3433±172	26	2011/06/26	78±1	46± 7	3779±771	30
2010/04/10	81±1	43± 8	3263±428	28	2011/06/27	78±2	49± 2	4455±171	32
2010/04/10	79±2	39± 5	3262±430	26	2011/06/28	79±2	53± 4	4292±599	35
2010/04/11	89±2	45± 9	4289±771	30	2011/07/01	93±1	44± 3	3090± 86	29
2010/04/11	86±2	40± 8	3262±257	26	2011/07/02	101±3	39± 2	2575± 86	26
2010/05/14	64±2	43± 6	3945±428	28	2011/07/27	60±3	43± 3	2746± 85	28

ent estimate we consider calibrations presented by McLure & Dunlop (2004), Greene & Ho (2005), Kaspi et al. (2005), Vestergaard & Peterson (2006), Shen et al. (2011), Vestergaard & Osmer (2009), and Decarli, Dotti, & Treves (2011). Average black hole masses estimated for each emission line are in Table 1, and in Figure 4 we compare the various recipes considered to determine these values. Our measurements are consistent with  $M_{\text{BH}} \sim 6 \times 10^8 M_{\odot}$ , regardless of the relation considered.

#### 4 SUMMARY AND CONCLUSIONS

We investigate the variability of broad lines of PKS 1222+216 through the analysis of spectra collected in a period of more than 3 years. The  $\text{H}\beta$  line remains almost unchanged despite multiple flaring in both optical and  $\gamma$ -rays. This is consistent with the scenario proposed by Tavecchio et al. (2011) in which the intense and rapidly variable VHE emission is located at large distance ( $\gtrsim 0.1$  pc) from the BLR (but see: Tavecchio et al. 2012).

Since the BLR emission is almost stable, we estimate the virial black hole mass following various recipes, and from Mg II,  $\text{H}\beta$  and  $\text{H}\alpha$ , we find that is  $\sim 6 \times 10^8 M_{\odot}$ . This mass is close to that proposed by Shen et al. (2011) on the basis of SDSS continuum which in fact corresponded to a low state, but it is significantly higher than the mass proposed by Wang, Luo, & Ho (2004) and reported by Tanaka et al. (2011). This possibly derives from Stockton & MacKenty (1987), where however no information is reported on the FWHM of  $\text{H}\beta$ .

The black hole mass of PKS 1222+216 does not substantially deviate from the mass distribution of the populations of FSRQ at the same redshift ( $0.1 \lesssim M_{\text{BH}}/10^8 M_{\odot} \lesssim 10.0$ , Shaw et al. 2012). Because of its redshift we expect that dedicated infrared observations of the source with a medium size telescope should enable the detection of the host galaxy, in particular in case of low optical-NIR emission activity: i.e. if the nuclear luminosity does not overcome the host galaxy luminosity by more than a factor of  $\sim 10$  (e.g., Kotilainen, Falomo, & Scarpa 1998; Meisner & Romani 2010; Kotilainen et al. 2011). From that an independent estimate of the black hole mass may follow.

#### ACKNOWLEDGEMENTS

We would like to thank the anonymous referee for his/her valuable and constructive comments. EPF acknowledge R. Scarpa for his support during observations at TNG.

For this work EPF was supported by Società Carlo Gavazzi S.p.A. and by Thales Alenia Space Italia S.p.A. RD acknowledges funding from Germany's national research centre for aeronautics and space (DLR, project FKZ 50 OR 1104). We acknowledge financial contribution from the agreement ASI-INAF I/009/10/0.

For this work we use: (i) observations made with the Italian Telescopio Nazionale Galileo (TNG) operated on the island of La Palma by the Fundación Galileo Galilei of the INAF (Istituto Nazionale di Astrofisica) at the Spanish Observatorio del Roque de los Muchachos of the Insti-

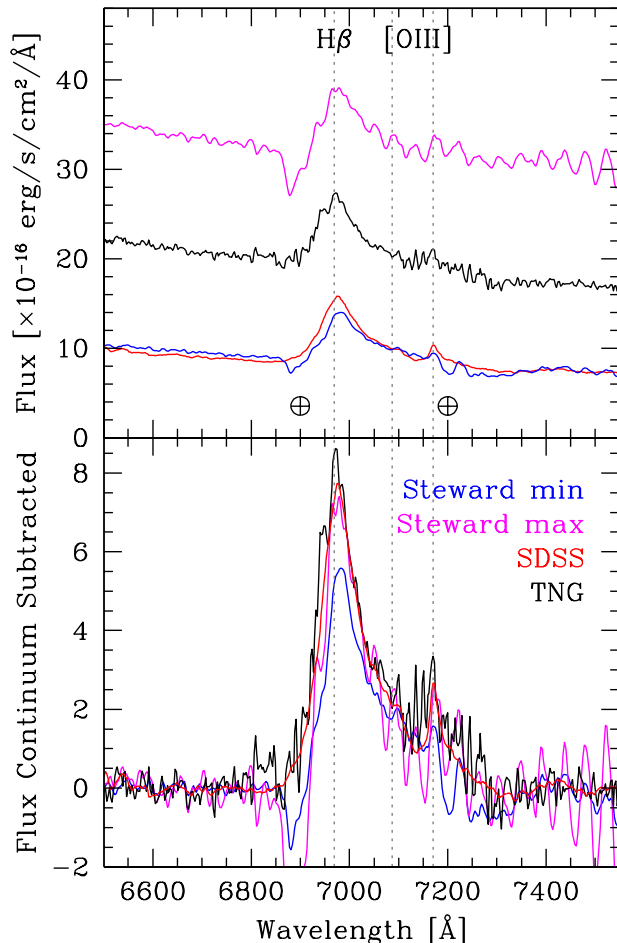


**Figure 3.** *Top Panel:* Zoom of the  $\text{H}\beta$  region of PKS 1222+216 spectra. Data are from SDSS (red line), TNG (black line) and Steward observatory at the minimum (blue line) and at the maximum (magenta line) of optical activity. The emission lines are marked with grey dotted vertical lines. The  $\oplus$  symbols point regions where the Steward observatory spectra are affected by telluric absorption. *Bottom Panel:* Same of the Top Panel but the spectra are continuum subtracted.

tuto de Astrofisica de Canarias; (ii) data from the Steward Observatory spectropolarimetric monitoring project were used, this program is supported by Fermi Guest Investigator grants NNX08AW56G and NNX09AU10G; (iii) data from the Sloan Digital Sky Survey. Funding for the SDSS and SDSS-II has been provided by the Alfred P. Sloan Foundation, the Participating Institutions, the National Science Foundation, the U.S. Department of Energy, the National Aeronautics and Space Administration, the Japanese Monbukagakusho, the Max Planck Society, and the Higher Education Funding Council for England. The SDSS Web Site is <http://www.sdss.org/>.

#### REFERENCES

- Aleksić J., et al., 2011, ApJ, 730, L8  
 Böttcher M., Reimer A., Marscher A. P., 2009, ApJ, 703, 1168

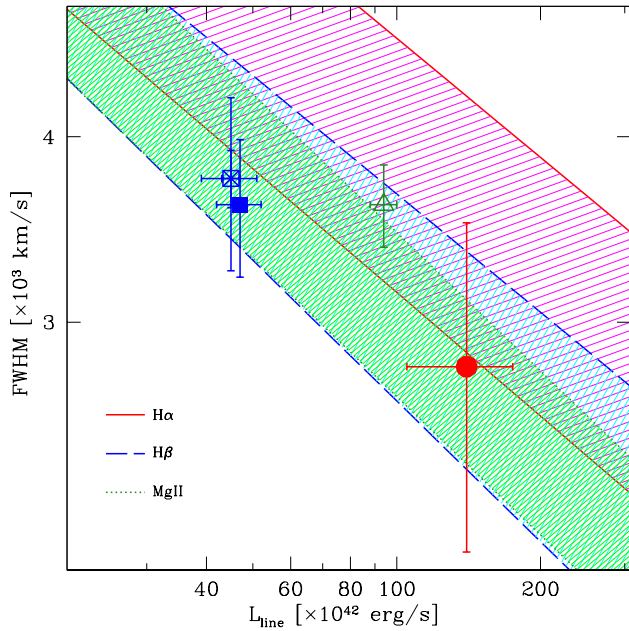


**Figure 4.** Relations between luminosity and FWHM of broad lines assuming a black hole with mass  $M_{\text{BH}} = 6 \times 10^8 M_{\odot}$ . Red plain, blue dashed, and green dotted lines include the different calibrations introduced in §3 for  $\text{H}\alpha$ ,  $\text{H}\beta$ , and  $\text{Mg II}$ , respectively. Red filled point is the measure of  $\text{H}\alpha$  from TNG spectra; blue points are the measure of  $\text{H}\beta$  from TNG (filled square), Steward (cross), and SDSS (empty square); the green empty triangle is the measure of  $\text{Mg II}$  from SDSS. A colour version of this figure is available in the electronic edition of MNRAS.

Burbidge E. M., Kinman T. D., 1966, *ApJ*, 145, 654  
 Brinkmann W., Yuan W., Siebert J., 1997, *A&A*, 319, 413  
 Carrasco L., Carramiñana A., Recillas E., Porras A., Mayya D. Y., 2010, *ATel*, 2626,  
 Ciprini S., 2009, *ATel*, 2349, 1  
 Decarli R., Labita M., Treves A., Falomo R., 2008, *MNRAS*, 387, 1237  
 Decarli R., Falomo R., Treves A., Kotilainen J. K., Labita M., Scarpa R., 2010, *MNRAS*, 402, 2441  
 Decarli R., Dotti M., Treves A., 2011, *MNRAS*, 413, 39  
 De Rosa G., Decarli R., Walter F., Fan X., Jiang L., Kurk J., Pasquali A., Rix H. W., 2011, *ApJ*, 739, 56  
 Donato D., 2010, *ATel*, 2584, 1  
 Greene J. E., Ho L. C., 2005, *ApJ*, 630, 122  
 Hartman R. C., et al., 1999, *ApJS*, 123, 79  
 Hauser M., Wagner S., Hagen H., 2010, *ATel*, 2436, 1  
 Hooimeyer J. R. A., Schilizzi R. T., Miley G. K., Barthel P. D., 1992, *A&A*, 261, 5  
 Iafrate G., Longo F., D’Ammando F., 2010, *ATel*, 2687, 1  
 Kaspi S., Maoz D., Netzer H., Peterson B. M., Vestergaard M., Jannuzi B. T., 2005, *ApJ*, 629, 61  
 Konigl A., 1981, *ApJ*, 243, 700  
 Kotilainen J. K., Falomo R., Scarpa R., 1998, *A&A*, 336, 479  
 Kotilainen J. K., Hyvönen T., Falomo R., Treves A., Uslenghi M., 2011, *A&A*, 534, L2  
 Longo F., Giroletti M., Iafrate G., 2009, *ATel*, 2021, 1  
 Mannucci F., Basile F., Poggianti B. M., Cimatti A., Daddi E., Pozzetti L., Vanzil L., 2001, *MNRAS*, 326, 745

Mariotti M., 2010, *ATel*, 2684, 1  
 McLure R. J., Dunlop J. S., 2004, *MNRAS*, 352, 1390  
 Meisner A. M., Romani R. W., 2010, *ApJ*, 712, 14  
 Molinari E., Conconi P., Pucillo M., 1997, *MmSAI*, 68, 231  
 Nalewajko K., Begelman M. C., Cerutti B., Uzdensky D. A., Sikora M., 2012, *arXiv*, arXiv:1202.2123  
 Nesci R., Montagni F., 2010, *ATel*, 2708, 1  
 Osterbrock D. E., Pogge R. W., 1987, *ApJ*, 323, 108  
 Raiteri C. M., Villata M., Lanteri L., Cavallone M., Sobrito G., 1998, *A&AS*, 130, 495  
 Schlegel D. J., Finkbeiner D. P., Davis M., 1998, *ApJ*, 500, 525  
 Smith P. S., Montiel E., Rightley S., Turner J., Schmidt G. D., Jannuzi B. T., 2009, *arXiv*, arXiv:0912.3621  
 Smith P. S., Schmidt G. D., Jannuzi B. T., 2011, *arXiv*, arXiv:1110.6040  
 Shaw M. S., et al., 2012, *arXiv*, arXiv:1201.0999  
 Shen Y., et al., 2011, *ApJS*, 194, 45  
 Stockton A., MacKenty J. W., 1987, *ApJ*, 316, 584  
 Striani E., et al., 2010, *ATel*, 2686, 1  
 Tanaka Y. T., et al., 2011, *ApJ*, 733, 19  
 Tavecchio F., Becerra-Gonzalez J., Ghisellini G., Stamerra A., Bonnoli G., Foschini L., Maraschi L., 2011, *A&A*, 534, A86  
 Tavecchio F., Roncadelli M., Galanti G., Bonnoli G., 2012, *arXiv*, arXiv:1202.6529  
 Urry C. M., Mushotzky R. F., 1982, *ApJ*, 253, 38  
 Urry C. M., Padovani P., 1995, *PASP*, 107, 803  
 Verrecchia F., et al., 2009, *ATel*, 2348, 1  
 Vestergaard M., Wilkes B. J., 2001, *ApJS*, 134, 1  
 Vestergaard M., Osmer P. S., 2009, *ApJ*, 699, 800  
 Vestergaard M., Peterson B. M., 2006, *ApJ*, 641, 689  
 York D. G., et al., 2000, *AJ*, 120, 1579  
 Wang J.-M., Luo B., Ho L. C., 2004, *ApJ*, 615, L9